Peer-reviewed version available at Atoms 2019, 7, 101; doi:10.3390/atoms7040101

Article

Tracking Temporal Development of Optical Thickness of Hydrogen Alpha Spectral Radiation in a Laser Induced Plasma

David M. Surmick [1] and Christian G. Parigger [2]

[1] Physics and Applied Physics, University of Massachusetts Lowell, Lowell, MA 01854; david_surmick@uml.edu
[2] Physics, University of Tennessee Space Institute, Tullahoma, TN 37388 2; cparigge@utsi.edu
* Correspondence: cparigge@tennessee.edu; Tel.: (931) 841-5690

Abstract: In this paper, we consider the temporal development of the optical density of the H_α spectral line in a hydrogen laser induced plasma. This is achieved by using the so-called duplication method in which the spectral line is re-imaged onto itself and the ratio of the spectral line with it duplication is taken to its measurement without the duplication. We asses the temporal development of the self-absorption of the H_α line by tracking the decay of duplication ratio from its ideal value of 2. We show that when 20% loss is considered along the duplication optical path length, the ratio is 1.8 and decays to a value of 1.25 indicating an optically thin plasma grows in optical density to an optical depth of 1.16 by 400 ns in the plasma decay for plasma initiation conditions using Nd:YAG laser radiation at 120 mJ per pulse in a 1.11×10^5 Pa hydrogen/nitrogen gas mixture environment. We also go on to correct the H_α line profiles for the self-absorption impact using two methods. We show that a method in which the optical depth is directly calculated from the duplication ratio is equivalent to standard methods of self-absorption correction when only relative corrections to spectral emissions are needed.

Keywords: atomic spectroscopy; radiation transfer; hydrogen; laser-induced breakdown spectroscopy; stark broadening

1. Introduction

The act of tightly focussing a laser beam of sufficient energy creates a dynamic, micro sized plasma. The temperature and density properties of the decaying plasma depend on the laser, focal, and ambient conditions used at the onset of the plasma. For a nominal nanosecond pulsed laser with 10-100 mJ of energy per pulse, this plasma can have a temperature range of 0.5 to 5 eV and an electron density range between 10^{15} and 10^{19} cm^{-3} depending on the plasma decay conditions and the laser ablation target [1]. Such plasma characteristics are ideal for use in nano-particle formation [2,3], pulsed laser deposition [4], and laser-induced breakdown spectroscopy (LIBS) [5–7]. In each of these applications optical spectroscopy becomes a primary tool (e.g., LIBS) for analysis and application, including use a tool for bench marking spectral line shapes with corresponding plasma conditions [8–10].

When the laser produced plasma is created, the hot and dense plasma state begins to cool and thermally expand. As this happens a cooler outer region of the plasma forms exterior to a hot plasma kernel. Radiation from this kernel is emitted through the plasma inner and outer regions along a particular line of sight. Along this line of sight, extinction of the radiation may occur and a spectroscopic line profile may become distorted resulting in absorption of the line [11]. For self-absorption, radiation

is emitted by a specific transition in the hot plasma core and is absorbed to the same transition existing in the region of the plasma. In the case of a typical LIBS plasma, the line shape is typically given as a Lorentzian line profile due to the Strong Stark broadening for these density ranges [12]. Alternatively, one can also model the line profile as a Voigt profile to include line shape contributions from the experimental apparatus and the relatively weak Doppler widths of spectral lines emitted in plasma with a temperature of the order of a few eV.

The impact of the absorption distortion on the line profile manifests in different ways depending on the amount of absorption. The tendency is for the line peak to flatten and broaden indicated by an increasing line width ($\Delta\lambda$) [13]. As the absorption becomes more extreme, the peak will take on a saturated form with a clear flat top peak and as the absorption becomes even more extreme the line will take on a reversed shaped with a clear central dip at the line center. This trend occurs for increasing optical depth τ and is displayed in Figure 1 for optical densities between 0 and 3. As can be seen, for moderate absorptions the line profile may not appear distorted (see τ=0.5 to 1). For applications such as quantitative LIBS where the line shape is pivotal for determining the plasma temperature and electron density [5], as well as determine elemental compositions from physical population [14] and univariate/multivariate models [5,15], distortions of the line profile need to be thoroughly addressed. Specific to the LIBS field of study, there is a long history of accounting for self-absorption [16–24]. Some methods depend on solving the equation of radiation transport[13,25–27], while others seek experimental corrections to specific line shapes of interest [23].

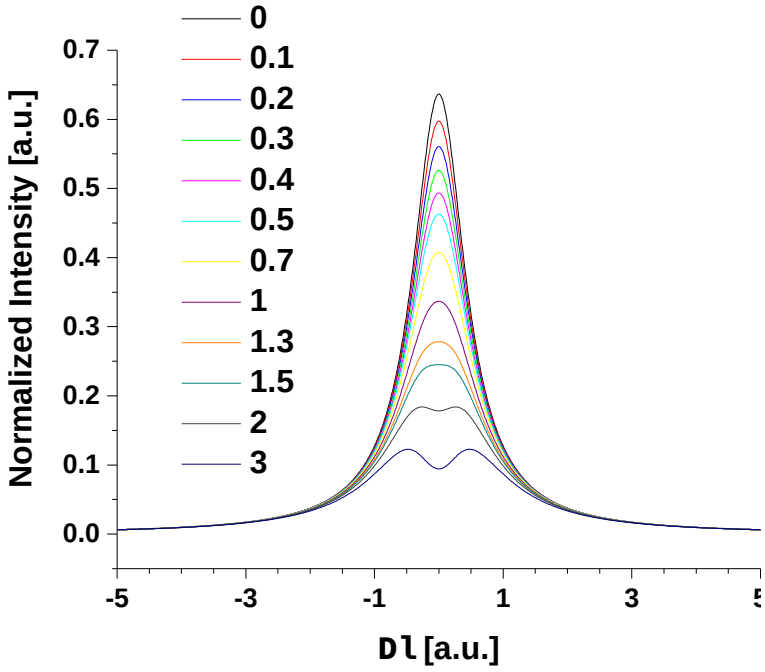

Figure 1. Alterations of a Lorentzian line profile under the influence of self-absorption for increasing optical density. The undistorted line width is 1 [a.u.].

In the present work, we detail the optical density of a laser induced plasma through out the plasma decay by monitoring the temporal progression of the hydrogen Balmer series α line (H_α). This is completed through the standard practice of using a doubling mirror to re-image the plasma onto itself and take ratios of the plasma spectroscopic image collected with and without its doubled image. In the following section, we detail the standard method for applying the doubling mirror method and suggest a potential alternative that requires less post processing of the measured spectra. We go on to apply both methods to measurements of the H_α line and use the corresponding electron density

determined from the line to indicate the usefulness of both methods of correcting the opacity of the spectral line.

2. Theory

The radiation transport equation details how light can be absorbed as it passes through a dense medium [11]. Specifically the amount of radiation ($L(\lambda, x)$) that leaves a column of absorbing material is detailed as

$$L(\lambda, x) = \epsilon(\lambda, x)dx - \kappa(\lambda, x)Ldx, \tag{1}$$

where $\epsilon(\lambda, x)$ the emission coefficient, $\kappa(\lambda, x)$ is the absorption along dx, and dx is a slab of absorbing material. A solution to the radiation transport equation when spatial homogeneity is assumed is given by

$$L(\lambda) = S(\lambda)(1 - e^{-\tau(\lambda)})\mathcal{L}(\lambda), \tag{2}$$

where $S(\lambda)$ is the source function, which is taken as the ratio of the emission and absorption coefficients ($\epsilon(\lambda)/\kappa(\lambda)$). $\mathcal{L}(\lambda)$ is the normalized line profile and τ is the optical depth, which is defined as

$$\tau(\lambda) = \int_0^{\ell} \kappa(\lambda)dx, \tag{3}$$

where ℓ is the size of the absorption path length. When the source is in local thermodynamic equilibrium the source function takes the form of the Planck function [28]. In order to account for absorption, one can rearrange Equation 2 to isolate the emission coefficient as

$$\epsilon(\lambda)\mathcal{L}(\lambda) = L(\lambda)\frac{\kappa(\lambda)}{1 - e^{-\tau(\lambda)}} \tag{4}$$

such that if one can calculate a correction factor, apart from a multiplication of ℓ, of the form

$$K(\lambda, \tau) = \frac{\tau}{1 - e^{-\tau(\lambda)}}, \tag{5}$$

absorption can be taken into account along a particular line of sight in a relative manner.

One methods for taking absorption into account is to duplicate the emission source with reflective optics and compare the original emission source to source with its duplication. In the case of laser induced plasma, duplication is typically done using some optical setup using a retro-reflecting mirror [8,22,23]. The retro-reflection is reduced by a factor of $e^{-\tau}$ as it passes through the original emission source such that the ratio of the reflection plus the original source to the original emission is

$$R(\lambda) = \frac{S(\lambda)(1 - e^{-\tau} + S(\lambda)(1 - e^{-\tau}G(\lambda)e^{-\tau})}{S(\lambda)(1 - e^{-\tau})}, \tag{6}$$

which reduces to

$$R(\lambda) = 1 + G(\lambda)e^{-\tau}, \tag{7}$$

where $G(\lambda)$ is a term that accounts for losses along the duplication optical path length. The method for tabulating a correction of the form of Equation 5 as outlined by Moon *et al.* [23] details using the ratio of the continuum with and without the emission duplication as a way of avoiding determining the optical losses, $G(\lambda)$. This method will hereafter be referred to the Kcorr method. In this scheme the correction factor is calculated as

$$K = \frac{\ln(y)}{y - 1}, \tag{8}$$

with

$$y = \frac{R_c(\lambda) - 1}{R(\lambda) - 1}, \tag{9}$$

where $R_c(\lambda)$ is the ratio of the continuum with and without the emission duplication. Rearranging 7 shows that the loss factor shifts the value of the τ that can be determined from direct division of the measured line profiles with and without the duplication mirror. Namely, for larger losses, smaller τ's and spectral intesnites are predicted.

As an alternative, we suggest directly finding $\tau(\lambda)$ from Equation 7 as simpler method of calculating $K(\lambda, \tau)$ in Equation 5. This removes the need to find the ratio of the line continuum and also removes the need to differentiate this continuum from the line spectrum. This alternative method does however require one to provide an estimation of the losses along the optical path length of the duplication imaging system. In the present work we will show that in a relative sense, the need for this estimation has little impact for relative spectroscopic measurements and analyses provided all lines used for analysis experience the same correction. The method will hereafter be referred to as the direct method of self-absorption correction.

3. Experimental Details

Laser-induced plasma was studied spectroscopically following plasma initiation from focused 1064 nm, Nd:YAG laser radiation. Self-absorption effects are studied by re-imaging the plasma onto itself prior to spectroscopic imaging through use of a plane, reflecting mirror. The plasma was initiated by focusing 120 mJ, 14 ns pulsed laser radiation through the window of a gas cell chamber. A 125-mm focal length UV-fused silica (UV-fs) planoconvex lens was used. The breakdown event was imaged onto the slit of a 0.64-meter Jobin-Yvon, HR640 Czerny Turner spectrometer installed with a 1200 grooves/mm grating. The gas cell was filled with 90% ultra-high purity (UHP, 99.999% pure) hydrogen gas and 10% UHP nitrogen gas and was evacuated with a mechanical/diffusion pump system to a pressure of 10^{-3} Pa (1×10^{-5} Torr) prior to filling the chamber volume with the desired gas mixture atmospheres. The chamber pressure at the time of the experiment was 1.11×10^{5} Pa (838 Torr).

The plasma emissions were recorded with an Andor iStar intensified charge couple device (ICCD). The detector was a rectangular array of pixels. When coupled with the spectrometer, the horizontal arrays of pixels are used to record spectrally resolved data. The vertical pixels on the detector recorded spatially resolved data along the height of the spectrometer slit. The laser was focussed vertically through the top of the chamber. The size of the ICCD pixels were 13.6 $\times$ 13.6 μm. This resulted gave a spectral instrument resolution of approximately 0.15 nm for the selected slit width of 50 microns. Groups of 8 vertical rows were data-binned to achieve a spatial instrument resolution of 0.108 mm along the slit height. The imaging characteristics of the system were such that the plasma imaged onto the ICCD at a magnification of 1.05:1. The spectral and spatial resolutions (or spectral and spatial instrument resolutions) are the important figures of merit, and for completeness we included the actual slit width that was used. The spectral resolution is determined by the slit width, the spatial resolution by the binning. Both of which are affected by the modulation transfer function, especially of the intensifier. The instrument resolution is determined by analyzing the line shapes of low temperature, low density stand lamp sources used for wavelength calibration.

Self-absorption was studied using a plane, reflecting mirror and a lens to reflect the plasma onto itself prior to spectroscopic imaging. The plasma was first imaged onto the plane reflecting mirror. This image was then passed back through the lens and onto the plasma. The plasma and its duplicate were then imaged onto the spectrometer slit as is usually done in a typical LIBS experiment [29]. A block diagram of the apparatus is shown in Figure 2. The lenses used to image the plasma onto the mirror and the plasma and its duplicate image onto the spectrometer slit were identical and consisted of uncoated, UV-fs singlets with a focal length of 100 mm. To aid in the alignment of the apparatus,

Preprints (www.preprints.org) | NOT PEER-REVIEWED | Posted: 2 October 2019 doi:10.20944/preprints201910.0013.v1

Peer-reviewed version available at Atoms 2019, 7, 101; doi:10.3390/atoms7040101

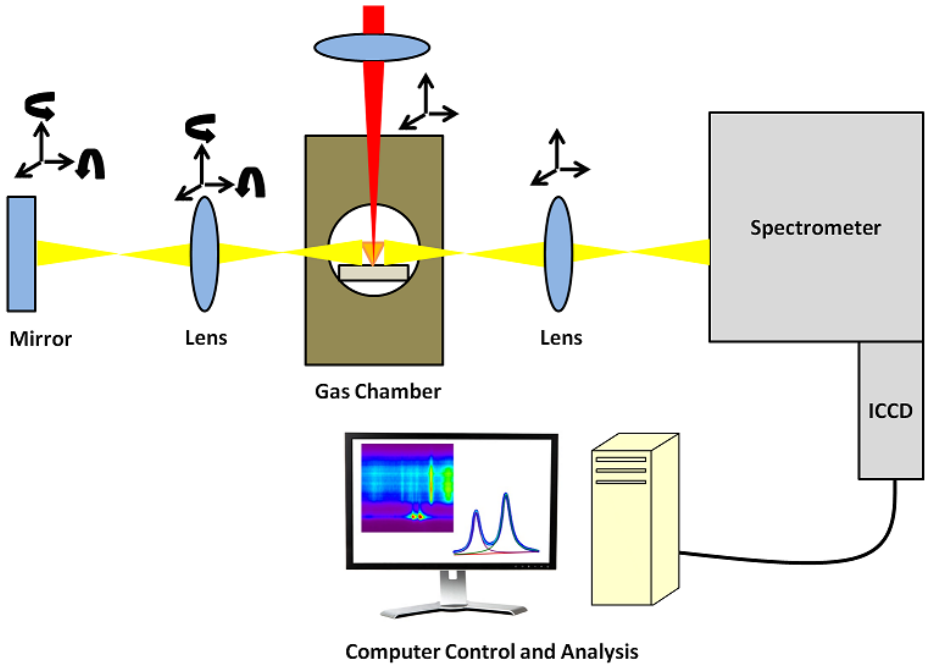

Figure 2. Block diagram of the experimental apparatus detailing self-absorption re-imaging.

the mirror and the lens used to image the plasma onto the mirror were positioned with 5-axis Gimbal mounts for fine adjustments.

The alignment of the self-absorption apparatus is a delicate and vital component of this work given the spatial resolution of the ICCD. To aid in this procedure, the lens used to image the plasma with its duplication was fixed in its position so that it properly produced a focused image on the spectrometer slit. This corresponded to the location equivalent to the distance of $2\times$ the focal length of the lens in relation to the spectrometer slit and $2\times$ the back focal length (93.7 mm) in relation to the breakdown plasma, when taking into account the thick-lens approximation. Likewise, the lens used to image the plasma onto the plane mirror was initially placed at a distance of twice the focal length of the lens in relation to the mirror and twice the back focal length of the lens in relation to the breakdown plasma. The best possible alignment was achieved by fine adjustments of both lenses and the mirror. The alignment was checked using zero order imaging with the spectrometer. A sufficient alignment was considered to be one in which ICCD images collected with and without the duplication were nearly identical. Further fine adjustments were made by comparing collected ICCD spectra with and without the duplication such that the ratio was as large as possible, with an ideal ratio limit of 2. These adjustments were made by viewing the Balmer series hydrogen beta line, H_β, at a time delay of 10 μs in SATP laboratory air breakdown. For this time delay, self-absorption for this spectral line is likely to be insignificant, especially in ambient air (as differentiated from the high pressure atmosphere used here) [30,31].

H_α spectra were recorded at systematically varied time delays starting from 10 ns following plasma initiation up to a delay of 2150 ns. The selected gate width for the first 100 ns was 5 ns and a 150 ns gate width was used for all later measurements. Temporal resolution was achieved by synchronizing the ICCD to the Q-Switch output of the laser. This image shows the spatial localization with respect to the slit height and wavelength range of the emitted spectra. Though spatial resolution was used for the initial measurement, all the H_α spectroscopic images were averaged after data collection to improve the signal quality and mitigate the impacts of a slight misalignment on the scale of the 0.1 mm spatial resolution along the vertical axis. This averaging excluded regions above and below the H_α emission where only signal noise was recorded. Prior to analysis the spectrum was wavelength and intensity calibrated using a hydrogen glow discharge lamp and halogen light source, respectively.

4. Results and Discussion

4.1. Temporal Self-absorption Behavior

Following collection and averaging of the H_α spectra both with and without the duplicating mirror, ratios of the doubled image to the non-doubled spectral image were calculated. The temporal development of the H_α spectra with and without the duplicating mirror is displayed in Figures 3 and 4 in the first 100 ns and at the later investigated times, respectively. The left image in each figure shows the spectra and the right image shows the spectra imaged with the duplication. These images show the rise in the intensity of the H_α line from the spectral continuum and its growth in intensity as the plasma cools and atomic recombination occurs. The spectra first become apparent after 30 ns as seen in Fig 3a. The H_α line is initially very broad but narrows gradually through time as the plasma decays. Prior to the 30-ns time delay, the plasma is characterized by strong continuum emissions. After reaching a peak intensity between 150 and 400 ns, the line begins to decay indicating the n=3 levels of the hydrogen atoms are depopulating closer to the ground level as the plasma decays further and the plasma cools.

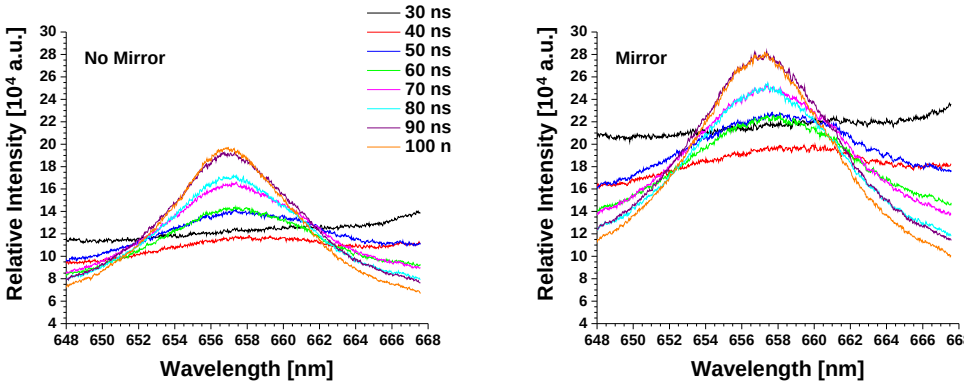

Figure 3. Temporal development of the H_α line in the first 100 ns following plasma initiation. The left image shows the measured spectra and the right image shows the spectra measured with its duplication.

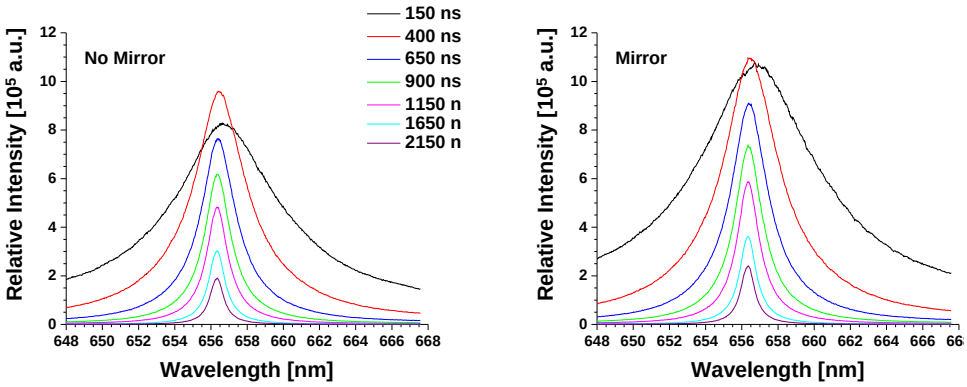

Figure 4. Temporal development of the H_α line between 150 ns and 2150 ns following plasma initiation. The left image shows the measured spectra and the right image shows the spectra measured with its duplication.

To determine the temporal profile of the self-absorption of the H_α line, the measurements with and without the H_α duplication were used in conjunction with Equation 5 by two methods: 1) Equations 8 and 9 are used by finding the ratio of the spectra with and without its duplication and also finding the

ratio of the continuum radiation for the Kcorr method and 2) by finding the optical depth according to Equation 7 and directly substituting this into the correction factor from Equation 5 for the direct method. Both methods rely on finding the ratio of the spectra collected with and without its duplication. To gain insight into the temporal development of the self-absorption, these ratios have been tracked through the plasma decay and are displayed in Figure 5, showing times between 30 and 2150 ns.

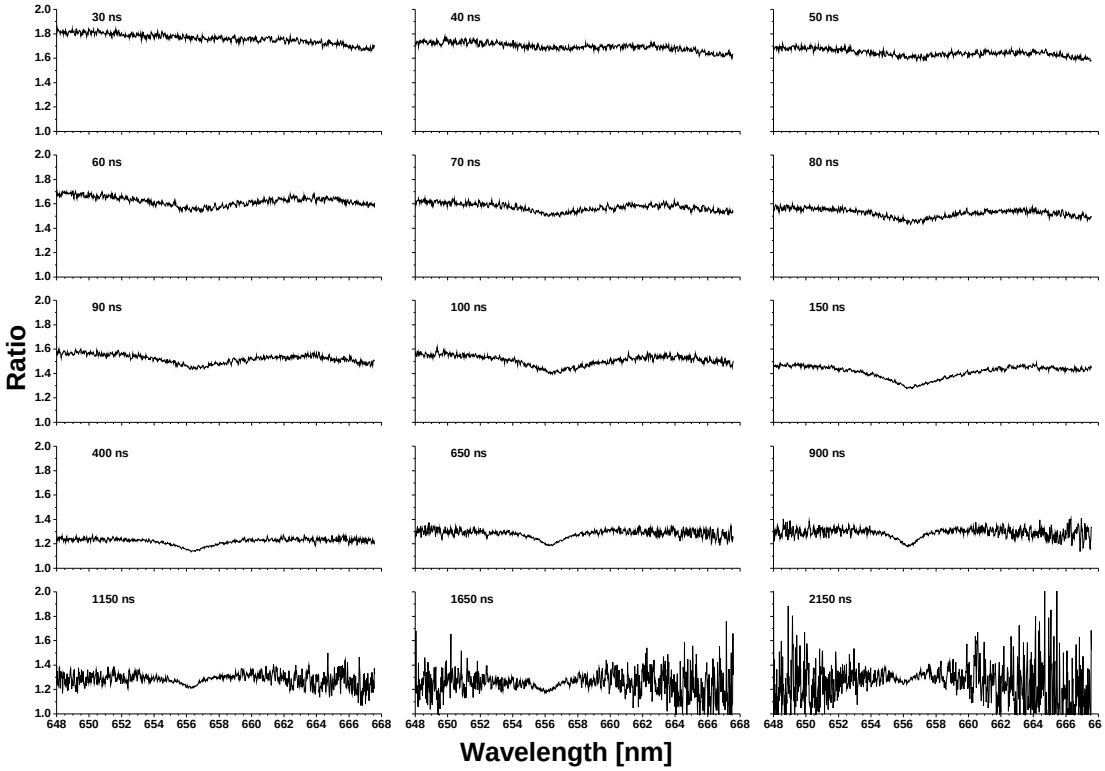

Figure 5. Ratios of the doubled H_α spectra to the non-doubled emissions through the plasma decay from 30 ns to 2150 ns. Each image has the wavelength and ratio ranges.

Initially, at 30 ns, the ratio is quite close to 2, the theoretical limit of the ratio. When losses are considered a value of the approaching or exceeding 1.8 indicates little to no line self-absorption, when the signal almost entirely a continuum signal. This would be consistent with a plasma model in which the approach atomic levels of hydrogen (n=2 and n=3 for the Balmer α line) are just beginning to populate. As the plasma decay continues these levels become more populated, as evidenced by the rise in intensity of the H_α line. As this goes on, the ratio of the H_α line with and without its duplication begins to steadily decrease. By 100 ns the value of the ratio is approximately 1.6 and reaches a maximum low of about 1.3 to 1.25 at time later than 400 ns. After this time, there is an apparent rise the ratio indicating the amount of extinction along the optical line of sight is reducing. However, the plateau in the decay of the ratio more than likely indicates that a limit in the sensitivity of the technique has been reached.

Figure 5 also shows the tendency for the line center to be more perturbed by self-absorption, as was shown in Figure 1. As the line absorption becomes more prominent, a dip in the ratio begins to appear near the H_α line center. This is first seen in at a time of 60 ns and grows in prominence as the plasma decays. The magnitude of the dip relative the mostly constant ratio in the line wings is between 0.05 to 0.1. Thus a minimum ratio of approximately 1.15 at the line center can be seen for the 400 ns time delay.

As the plasma decays, the line becomes more susceptible to experimental noise. The impact of this is amplified by dividing two spectra giving rise to the extreme noise seen in the ratios calculated after 800 ns. This noise addition can also be attributed to the narrowing nature of the H_α line as the

wings of the later time ratios are most impacted. In this case the wings represent a part of the spectrum that is characterized by an also decaying spectral continuum that will largely be the same between spectra collected with and without the duplication. Furthermore, this weakly intense continuum is more susceptible to noise contributions which is further amplified when the ratio is taken. This would also manifest in the early investigated times prior to 150 ns, the H_α line has contributions beyond the spectral range of our instrument, making it difficult to asses the contributions of the continuum radiation.

As a reference, Figure 6 shows the relationship between optical depth and the ratio of the spectral line with and without its duplication and without any losses given by Equation 5. At zero optical depth, the ratio is 2. As the optical depth increases to values greater than 1 ($\tau = 1$ is often cited as being optically thick [11]) the ratio approaches a limit of 1 indicating no radiation has emerged from the source. An optical depth of 1 corresponds to a ratio of nearly 1.37. Figure 5 suggests that a ratio of 1.25 in the line wings and 1.15 at line center can be extracted. This corresponds to optical depths of 1.38 and 1.89 at the line wings and line center, respectively, when no losses are considered. This is however an idealization that doesn't match the experimental conditions. If one were to assume a modest amount of loss along the duplication optical path length, such as 20% which means there is 93% transmittance all interfaces along duplication optical path, the optical depths become 1.16 and 1.67 at the line wings and line center, respectively. With a loss of 20% the ratio of 1.8 corresponds to an optically thin source. The increase in self-absorption as the plasma cools and decays has been reported in other studies as well [21,32,33].

Discussions of self-reabsorption [34] indicate that for an optically thin plasma and an ideal doubling mirror in place, the transmitted intensity amounts to twice that without the mirror. However, when the plasma is optically thick (at line center $\kappa_0 x \gg 1$) and for a Voigt parameter, a, or the ratio of Lorentzian and of Gaussian widths, $a \gg 1$, the line absorption, A_L, amounts to $A_L = 2 - \sqrt{2} = 0.59$. In other words, the transmission equals $\sqrt{2}$, i.e., 1.41 is the limiting value for the transmission. This results has been extensively communicated [35] and applied in the modeling of flame experiments [36] that utilize an experimental arrangement comprised of two consecutive line sources.

4.2. Self-absorption Impact on Line Shapes

The impact of the self-absorption on the temporal development is further discussed by applying the correction factor given in Equation 5 in two ways. The first is to use the Kcorr method outlined by Moon *et al.*[23]. In performing this method, the ratios from Figure 5 are used but they have been smoothed with a second order Savitzky-Golay filter with a window size of 50 in order to reduce the impact of noise on the corrected spectra. The ratio of the continuum was estimated by averaging the spectral end points on the desired range. These points were 645.5 and 667.547 nm. When the H_α line is sufficiently narrow ($\Delta\lambda = $ 4nm) these points indicate a distance from line center that is 5$\times$ the line width, which provides a reasonable continuum estimation that is uninhibited by the H_α line profile. When the line is at its widest, these points are only 2$\times$ the line width which introduces some uncertainty in determining the ratio of the continuum and also represents a limit of this method for narrow band spectra with broad spectral features.

The second method of correction is directly invert Equation 7 to find the optical depth using the ratios given in Figure 5 for the direct method. The ratios are once again smoothed using the Savitzky-Golay filter. With this method one either needs to have an accurate characterization of the optical losses along the duplication optical path length or assume a reasonable loss. Characterizing the loss along duplication optical path length could be an arduous task that involves considering the modulation transfer function and other geometric optics impacts to determine the imaging system quality. At this stage, rather than take on this task, we instead consider three values of a loss to gauge the efficacy of using this method to correct the H_α spectra in a relative sense. The losses we consider include: No loss (an unlikely ideal case), 10% loss, and 20% loss. For use in Equation 7, these values

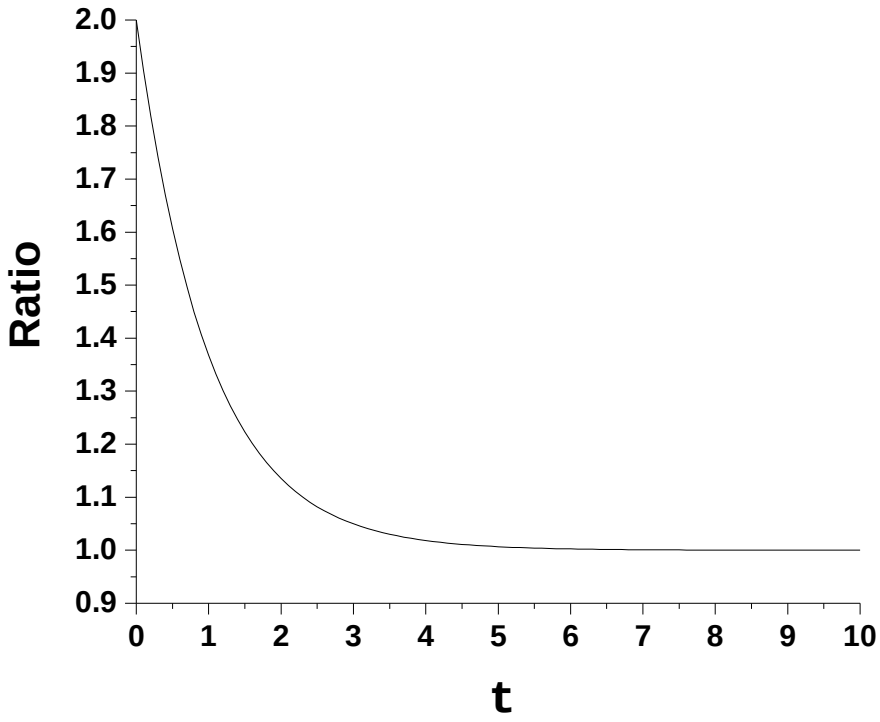

Figure 6. Relationship between optical depth, τ, and the ratio of a spectral line with its duplication compared to the line without duplication.

correspond to constant $G(\lambda)$ values of 1, 0.9, and 0.8. It is also reasonable to assume that the loss on a narrow spectral band of 22 nm is relatively constant.

Using three different values of the loss allows us to see how the line shape is impacted changing this parameter which will be important for further studies using this method of self-absorption correction. The no loss and 10% loss cases are likely ideal scenarios that would be difficult to experimentally achieve. The 20% loss case represents a best case scenario in which the optical system is perfectly aligned and highly efficient optics at the H_α wavelength are considered with a transmittance near 0.93 at each optical interface on the duplication optical path. After the loss is accounted for, the line profiles are now corrected using Equation 5 with the tabulated optical depths.

Figure 7 shows the result of applying both methods of correcting the H_α line at 100 and 600 ns time delays. For comparison, the measured line profile without its duplication is also presented. The most notable aspect of applying the two different methods is the Kcorr method produces a spectrum that is more comparable in intensity with the original line profile, however, the corrected line profile is now narrower (at both time delays) as would be expected. When the direct method as the self-absorption correction, the line intensity grows. The amount of intensity growth depends on the amount of loss. The greater the loss, the less the intensity of the line grows. The spectral features for each of the considered losses do appear to be narrower after correction, however.

Despite the line growth when the lines are corrected according to the direct method, the spectral intensities that are observed are relative in nature, as only a relative intensity correction of the experimental apparatus was performed. This is a common practice as absolute calibrations of spectral imaging systems are difficult to perform and are not necessary in most cases since quantitative information can be extracted from a relative intensity correction. For example, the line shape would only be impacted by an amplitude factor. Provided this amplitude factor is self consistent across an entire spectrum the quantitative analysis is not impacted. For the method at hand, provided it can

Preprints (www.preprints.org) | NOT PEER-REVIEWED | Posted: 2 October 2019 doi:10.20944/preprints201910.0013.v1

Peer-reviewed version available at Atoms 2019, 7, 101; doi:10.3390/atoms7040101

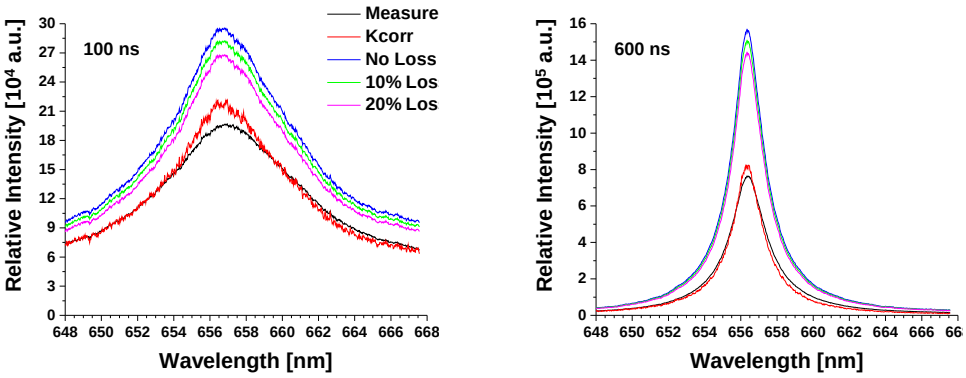

Figure 7. Results of correcting the H_α spectrum using the methods of Equation 8 and 9 and also directly calculating the optical depth with assumed losses in conjunction with Equation 7 for 100 ns (left) and 400 ns (right) time delays in the plasma decay.

be applied to multiple lines self consistently, further methods should not be impacted, though one should perform a baseline study for each new type of analysis that is considered (Boltzmann plots, multivariate modeling, *etc.*).

To compare the two methods of self-absorption correction and verify the line profile remain unaltered regardless of the method, the uncorrected and corrected line profiles were fit in order to calculate the line width. The line width was used to calculate the electron density to see the impact on determining the plasma state. The line profiles were fit with a Voigt line profile, an integral line shape function resulting from the convolution of Lorentzian and Gaussian line shapes [11]. The Lorentzian component of the Voigt profile represents the Stark broadened H_α line, while the Gaussian component represents in the instrument function width of 0.15 nm (determined during spectrometer-detector calibration) under the assumption of negligible Doppler broadening. One should note that the exact line shape of a Stark broadened hydrogen Balmer series line is a Holtsmarkian line profile, however for ease of analysis the Lorentzian line profile is an acceptable approximation [37–39].

The integral Voit line profile is numerical calculated using Fadeeva function or also called complex complimentary error function with the fixed Gaussian width of 0.15 nm [40,41]. The line profile fitting was implemented in the MatLab scripting environment [42]. The Fadeeva function was numerically calculated using the Algorithm 916 method of Zaghloul *et al.* [43]. Line shape fitting was carried using a Trust Region nonlinear curve fitting routine [44,45] in which the fit parameters were the line width, amplitude, and shift as well as two terms used characterize a linear offset to model any continuum components in the spectra signals.

In terms of characterizing the electron density of the plasma, one typically uses the line width. As a result, the behavior of the width before and after the self-absorption corrections is considered. These results are displayed in Table 1 and detail the line width progression from 40 ns to 2150 ns. The 30 ns time is left out from this discussion because the H_α line has not yet emerged from the spectral continuum. The table shows the what the uncorrected line width would be and the corrected line widths using The Kcorr and direct methods with no, 10%, and 20% losses. The table shows that initially the H_α line is very broad ($\Delta\lambda > 9\,\text{nm}$) and subsequently decays to a relatively narrow line ($\Delta\lambda < 1\,\text{nm}$). The uncertainties on the indicated line widths represent contributions from both the minimum spectral resolution and uncertainties introduced during line profile fitting. These uncertainties are greatest when the line is at its broadest and decay to a minimum value of 0.15 nm representing little to no uncertainty contribution from the fitting algorithms. This occurs after 400 ns when the line width is less than 4 nm and 5$\times$ the line width occurs on the investigated spectral range, indicating the spectral continuum is likely to be well characterized within the measurement.

Table 1 shows that regardless of the method of correcting the spectrum, the line width is reduced when the self-absorption factor is applied. The reduction in line widths ranges from 9 to 3.5 percent

Table 1. Line widths of the H_α line prior to and after self-absorption correction using all the stated methods. The 30 ns time delay is excluded form the table because the H_α has not yet emerged from the continuum at this point.

Time [ns]	Uncorrected $\Delta\lambda$ [nm]	Kcorr $\Delta\lambda$ [nm]	No Loss $\Delta\lambda$ [nm]	10% Loss $\Delta\lambda$ [nm]	20% $\Delta\lambda$ [nm]
40	8.42 ± 0.34	7.33 ± 0.43	6.80 ± 0.34	6.77 ± 0.34	6.74 ± 0.34
50	9.80 ± 0.28	9.01 ± 0.28	8.89 ± 0.25	8.88 ± 0.25	8.86 ± 0.25
60	9.24 ± 0.23	8.32 ± 0.23	8.20 ± 0.23	8.19 ± 0.23	8.17 ± 0.23
70	8.98 ± 0.26	8.12 ± 0.21	8.03 ± 0.21	8.01 ± 0.22	7.99 ± 0.21
80	8.57 ± 0.24	7.63 ± 0.19	7.64 ± 0.20	7.61 ± 0.20	7.60 ± 0.20
90	8.11 ± 0.21	7.34 ± 0.19	7.31 ± 0.19	7.30 ± 0.19	7.29 ± 0.19
100	7.80 ± 0.20	6.93 ± 0.18	6.93 ± 0.18	6.92 ± 0.18	6.90 ± 0.18
150	6.30 ± 0.17	5.46 ± 0.16	5.51 ± 0.16	5.49 ± 0.16	5.47 ± 0.16
400	3.72 ± 0.15	3.17 ± 0.15	3.28 ± 0.15	3.28 ± 0.15	3.27 ± 0.15
650	2.53 ± 0.15	2.19 ± 0.15	2.27 ± 0.15	2.26 ± 0.15	2.25 ± 0.15
900	1.88 ± 0.15	1.58 ± 0.15	1.66 ± 0.15	1.66 ± 0.15	1.65 ± 0.15
1150	1.51 ± 0.15	1.36 ± 0.15	1.40 ± 0.15	1.40 ± 0.15	1.40 ± 0.15
1650	1.10 ± 0.15	1.02 ± 0.15	1.04 ± 0.15	1.04 ± 0.15	1.04 ± 0.15
2150	0.90 ± 0.15	0.57 ± 0.15	0.87 ± 0.15	0.87 ± 0.15	0.87 ± 0.15

from the early times to the later plasma decay times, respectively. Furthermore, the two methods of correcting for the self-absorption return similar values of the line width after correction. The amount of loss considered in the relative correction model also produces similar line widths. Early in the plasma decay the Kcorr methods tends produce line widths that are 0.1 nm greater than the Equation 7 method. This can be attributed to the difficulty in appropriately finding the continuum ratio when the line is still very broad.

When the uncertainties are considered, the line widths can be considered to be the same for both methods of self-absorption correction and all three losses considered. There are two exceptions when the Kcorr value does not match the direct method. At 40 ns, the Kcorr method is 0.5 nm greater, yet there is a slight overlap when the uncertainties are considered. At this time, the H_α, while noticeable, is still emerging from the continuum and is also very broad making it difficult to ascertain the ratio of the continuum. This point was also the most uncertain in terms of the line profile fitting. The second point with a notable discrepancy is the 2150-ns time delay value for Kcorr. At this time the value of the ratio of the continuum is also difficult to ascertain due to the decaying nature of the plasma. As the plasma decays this value will tend toward unity which causes a singularity in the expression for Kcorr in Equation 8. This represents and advantage of the method using Equation 7 directly, as less processing of the spectra is required in order to obtain a correction factor. With the fact that the line profile is preserved in a relative sense one may prefer this method even though an estimate of the loss along the duplication optical path is required.

The final investigation of this work is to consider the electron density, N_e, decay of the plasma. This is shown in Figure 8 along with the line width decay of the H_α line. The N_e was determined H_α line width using the empirical formula outlined in Reference [46]. For the H_α line, the N_e is approximately proportional to $\Delta\lambda^{2/3}$ [37,38,46,47]. This figure mimics the results shown in Table 1. The line widths and electron densities are reduced when each of the self-absorption correction methods are applied and the each of the corrected densities and line widths agree with each other, especially when the uncertainty is considered. The impact of not accounting for self-absorption, even when moderate is clear from Figure 8. The electron density can be over estimated. For quantitative analysis, such as calibration free LIBS, this can alter the elemental compositions that are determined, over and beyond any impact that the line shape distortion may cause. Also as expected, the plasma is seen decay in density as the plasma cools and atomic and molecular recombination occurs. The plasma is seen to decay from an electron density of approximately 2×10^{18} cm^{-3} at 50 ns to approximately 5×10^{16} cm^{-3} at 2150 ns, following some manner of exponential decay as one might expect.

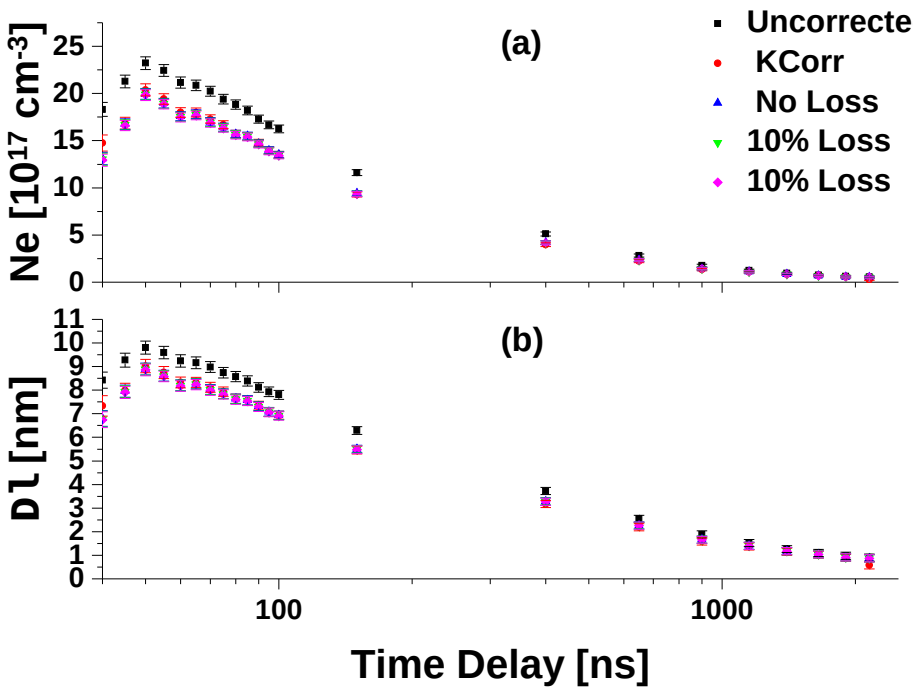

Figure 8. Decay of the plasma **(a)** electron density and **(b)** H_α line width through time.

5. Conclusions

In this work, the temporal development of the self-absorption of the H_α line was considered by studying the duplication method of re-imaging the spectral line onto itself and comparing the line with and without this duplication. The temporal development of this ratio indicated that the early stages of the plasma decay there is little self-absorption occurring in the plasma as the ratio value was 1.8. Throughout the plasma decay this value reduced to a minimum of 1.25 indicating an optical depth of 1.16 when a loss of a 20% is considered along the duplication optical path length. This result showed that as the plasma decayed and cooled the appropriate levels of hydrogen became sufficiently populated to induce self-absorption of the spectral line even if it is not readily obvious via visual inspection of the line profile.

The spectral line profiles were then corrected using two methods. The first was the standard method outlined by Moon *et al.* [23]. The second involved a direct calculation of the optical depth from the ratios of the spectra measured with and without its duplication. This required the assumption of some form of loss along the duplication optical path length. Investigation of the corrected profiles using line profile fitting methods with an emphasis on preserving the line width showed that both methods corrected the line self-absorption equally by finding the same line width within experimental uncertainty. The amount of loss considered along the duplication optical path only impacted the intensity of the signal, such that in an experiment where only relative intensities are required either method of self-absorption correction may be considered.

Author Contributions: All authors contributed equally to this work.

Funding: This research received no external funding.

Acknowledgments: The authors wish to acknowledge the support of the Center for Laser Applications at the University of Tennessee Space Institute for partial support of the experimental work of this effort.

Conflicts of Interest: The authors declare no conflict of interest.

References

1. Parigger CG. Atomic and molecular emissions in laser-induced breakdown spectroscopy. Spectrochim. Acta Part B: At. Spectrosc. 2013;79-80:4 – 16.
2. Harilal SS, Brumfield BE, Cannon BD, Phillips MC. Shock wave mediated plume chemistry for molecular formation in laser ablation plasmas. Anal. Chem. 2016;88:2296–2302.
3. Lam J, Amans D, Chaput F, Diouf M, Ledoux G, Mary N, Masenelli-Varlot K, Motto-Ros V, Dujardin C. γ-Al_2O_3 nanoparticles synthesized by pulsed laser ablation in liquids: A plasma analysis. Phys. Chem. Chem. Phys. 2016;16:963–973.
4. Panda AK, Singh A, Thirumurugesan R, Kuppusami P, Mohandas E. Optimization of substrate-target distance for pulsed laser deposition of tungsten oxide thin films using Langmuir probe. J. Instrument. 2015;10(09):P09014.
5. Cremers DA, Radziemski LJ. Handbook of Laser-Induced Breakdown Spectroscopy. Hoboken, NJ: John Wiley and Sons; 2006.
6. Hahn DW, Omenetto N. Laser-Induced Breakdown Spectroscopy (LIBS), Part 1: Review of Basic Diagnostics and Plasma-Paritcle Interactions: Still-Challeneging Issues Within the Analytical Plasma Community. Appl. Spectrosc. 2010;64:335A–366A.
7. Hahn DW, Omenetto N. Laser-Induced Breakdown Spectroscopy (LIBS), Part II: Review of Instrumental and Methodological Approaches to Material Analysis and Applications to Different Fields. Appl. Spectrosc. 2012;66:347–419.
8. Konjevic N. On the use of non-hydrogenic spectral line profiles for plasma electron density diagnostics. Plasma Sources Sci. Technol. 2001;10:356–363.
9. Konjevic N, Dimitrijevic MS, Wiese WL. Experimental stark widths and shifts for spectral lines of neutral atoms: A critical review of selected data for the period 1976 to 1982. J. Phys. Chem. Ref. Data. 1984;13:649–686.
10. Konjevic N, Dimitrijevic MS, Wiese WL. Experimental stark widths and shifts for spectral lines of positive ions: A critical review of selected data for the period 1976 to 1982. J. Phys. Chem. Ref. Data. 1984;13:619–647.
11. Kunze HJ. Introduction to Plasma Spectroscopy. Berlin, Heidelberg: Springer-Verlag; 2009.
12. Griem HR. Spectral Line Broadening By Plasmas. New York: Academic Press; 1974.
13. Cowan RD, Dieke GH. Self-Absorption of Spectrum Lines. Rev. Mod. Phys. 1948;20:418–455.
14. Cristoforetti G, Giacomo AD, Dell'Aglio M, Legnaioli S, Tognoni E, Palleschi V, Omenetto N. Local Thermodynamic Equilibrium in Laser-Induced Breakdown Spectroscopy: Beyond the McWhirter criterion. Spectrochim. Acta Part B: At. Spectrosc. 2010;65:86 – 95.
15. Gottfried JL. Discrimination of biological and chemical threat simulants in residue mixtures on multiple substrates. Anal. Bioanal. Chem. 2011;400(10):3289–3304.
16. Amamou H, Bois A, Ferhat B, Redon R, Rossetto B, Matheron P. Correction of self-absorption spectral line and ratios of transition probabilities for homogeneous and LTE plasma. J. Quant. Spectrosc. Radiat. Transf. 2002;75(6):747 – 763.
17. Amamou H, Bois A, Ferhat B, Redon R, Rossetto B, Ripert M. Correction of the self-absorption for self-reversed spectral lines: Application to two resonance lines of nuetral aluminium. J. Quant. Spectrosc. Radiat. Transf. 2003;77:362–372.
18. Bulajic D, Corsi M, Cristoforetti G, Legnaioli S, Palleschi V, Salvetti A, Tognoni E. A procedure for correcting self-absorption in calibration free-laser induced breakdown spectroscopy. Spectrochim. Acta Part B: At. Spectrosc. 2002;57:339 – 353.
19. Burger M, Skočić M, Bukvić S. Study of self-absorption in laser induced breakdown spectroscopy. Spectrochim. Acta Part B: At. Spectrosc. 2014;101:51 – 56.
20. El Sherbini AM, El Sherbini TM, Hegazy H, Cristoforetti G, Legnaioli S, Palleschi V, Pardini L, Salvetti A, Tognoni E. Evaluation of self-absorption coefficients of aluminum emission lines in laser-induced breakdown spectroscopy measurments. Spectrochim. Acta Part B. At. Spectrosc. 2005;60:1573–1579.
21. Fu Y, Warren RA, Jones WB, Smith BW, Omenetto N. Detecting Temporal Changes of Self-Absorption in a Laser-Induced Copper Plasma from Time-Resolved Photomultiplier Signal Emission Profiles. Appl. Spectrosc. 2019;73(2):163–170.

22. Herrera KK, Tognoni E, Omenetto N, Smith BW, Winfordner JD. Semi-quantitative analyis of metal alloys, brass and soil samples by calibration-free laser-induced breakdown spectroscopy: Recent results and considertions. J. Anal. At. Spectrom. 2009;24:413–425.
23. Moon HY, Herrera KK, Omenetto N, Smith BJ, Winefordner JD. On the usefulness of a duplicating mirror to evaluate self-absorption effects in laser induced breakdown spectroscopy. Spectrochim. Acta Part B: At. Spectrosc. 2009;64:702–713.
24. Omenetto N, Winefordner JD, Alkemade CTJ. An expression for the atomic flourescence and thermal-emission intensity under conditions of near saturation and arbitrary self-absorption. Spectrochim. Acta Part B: At. Spectrosc. 1975;30:335–341.
25. Hermann J, Grojo D, Axente E, Gerhard C, Burger Mcv, Craciun V. Ideal radiation source for plasma spectroscopy generated by laser ablation. Phys. Rev. E. 2017;96:053210.
26. Gornushkin IB, Stevenson CL, Smith BW, Omenetto N, Winefordner JD. Modeling an inhomogeneous optically thick laser induced plasma: a simplified theoretical approach. Spectrochim. Acta Part B: At. Spectrosc. 2001;56(9):1769 – 1785.
27. Hermann J, Boulmer-Leborgne C, Hong D. Diagnostics of the early phase of an ultraviolet laser induced plasma by spectral line analysis considering self-absorption. J. Appl. Phys. 1998;83(2):691–696.
28. Bransden BH, Joachain CJ. Physics of atoms and molecules. 2nd ed. New York: Prentice Hall; 2003.
29. Parigger CG, Woods AC, Witte MJ, Swafford LD, Surmick DM. Measurement and analysis of atomic hydrogen and diatomic molecular AlO, C_2, CN, and TiO spectra following laser-induced optical breakdown. J. Vis. Exp. 2012;38:E51250.
30. Ivković M, Konjević N, Pavlović Z. Hydrogen Balmer beta: The separation between line peaks for plasma electron density diagnostics and self-absoprtion test. J. Quant. Spectrosc. Radiat. Transf. 2015;154:1–8.
31. Gautm G, Surmick DM, Parigger CG. Comment on "Hydrogen Balmer beta: The separation between line peaks for plasma electron density diagnsotics and self-saborption test". J. Quant. Specrosc. Radiat. Transf. 2015;160:19–21.
32. Aguilera JA, Aragón C. Characterization of laser-induced plasmas by emission spectroscopy with curve-of-growth measurements. Part I: Temporal evolution of plasma parameters and self-absorption. Spectrochim. Acta Part B: At. Spectrosc. 2008;63:784 – 792.
33. Gornushkin IB, Anzano JM, King LA, Smith BW, Omenetto N, Winefordner JD. Curve of growth methodology applied to laser-induced plasma emission spectroscopy. Spectrochim. Acta Part B: At. Spectrosc. 1999;54(3):491 – 503.
34. Fujimoto T. Plasma Spectroscopy. Oxford: Clarendon-Press; 2004.
35. Ladenburg R, Reiche F. Über selective Absorption. Ann. Phys. 1913;347(11):181 – 209.
36. Gouy GL. Recherches Photométrigues sur les Flammes Colorées. Ann. Chim. Phys. 1879;18(5):5 – 101.
37. Gigosos MA, Gonzalez MA, Cardenoso V. Computer simulated Balmer-alpha, -beta, and -gamma Stark line profiles for non-equilibirum plasma diagnostics. Spectrochim. Acta Part B: At. Spectrosc. 2003;58:1489–1504.
38. Konjević N, Ivković M, Sakan N. Hydrogen Balmer lines for low electron number density plasma diagnostics. Spectrochim. Acta Part B: At. Spectrosc. 2012;76:16 – 26.
39. Parigger CG, Plemmons DH, Oks E. Balmer series Hβ measurements in a laser-induced hydrogen plasma. Appl. Opt. 2003;42(30):5992–6000.
40. Abramowitz M, Stegun IA. Handbook of mathematical functions with formulas, graphs, and mathematical tables. 9th ed. New York: Dover; 1964.
41. Fadeeva V, Terentjev NM. Tables of values of the proability integral for complex arguments. Moscow: State Publishing House for Technical and Technological Literature; 1954.
42. MatLab 2018a TM. Natick, MA; 2018.
43. Zaghloul MR, Ali AN. Algorithm 916: Computing the Faddeyeva and Voigt functions. ACM Trans. Math. Soft. 2011;38:15:1–15:22.
44. Byrd RH, Schnabel RB, Schultz GA. A trust region algorithm for nonlinearly constrained optimization. SIAM J. Numer. Anal. 1987;24:1152–1170.
45. Coleman TF, Li Y. An Interior Trust Region Approach for Nonlinear Minimization Subject to Bounds. SIAM J. Optimiz. 1996;6:418–445.
46. Surmick DM, Parigger CG. Empirical Formulae for Electron Density Diagnostics from Hα and Hβ Line Profiles. Int. Rev. At. Mol. Phys. 2014;5:73–81.

468 47. Griem HR, Halenka J, Olchawa W. Comparison of hydrogen Balmer-alpha Stark profiles measured at high
469 electron densities with theoretical results. J. Phys. B: At. Mol. Opt. Phys. 2005;38(7):975.